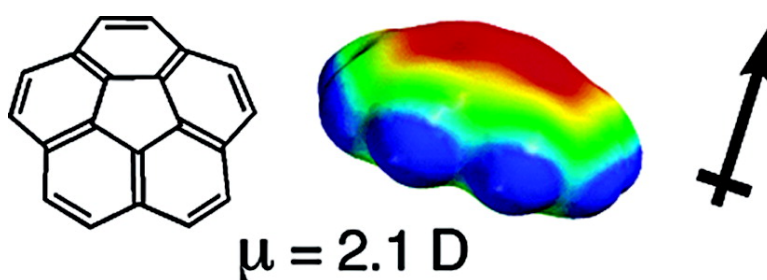


Interstellar Chemistry: A Strategy for Detecting Polycyclic Aromatic Hydrocarbons in Space

F. J. Lovas, Robert J. McMahon, Jens-Uwe Grabow, Melanie Schnell, James Mack, Lawrence T. Scott, and Robert L. Kuczkowski

J. Am. Chem. Soc., **2005**, 127 (12), 4345-4349 • DOI: 10.1021/ja0426239 • Publication Date (Web): 08 March 2005

Downloaded from <http://pubs.acs.org> on March 24, 2009



More About This Article

Additional resources and features associated with this article are available within the HTML version:

- Supporting Information
- Links to the 7 articles that cite this article, as of the time of this article download
- Access to high resolution figures
- Links to articles and content related to this article
- Copyright permission to reproduce figures and/or text from this article

[View the Full Text HTML](#)



Interstellar Chemistry: A Strategy for Detecting Polycyclic Aromatic Hydrocarbons in Space

F. J. Lovas,[†] Robert J. McMahon,^{*,‡} Jens-Uwe Grabow,[§] Melanie Schnell,[§]
James Mack,^{#,§} Lawrence T. Scott,[#] and Robert L. Kuczkowski[⊥]

Contribution from the Optical Technology Division, National Institute of Standards and Technology, Gaithersburg, Maryland 20899, Department of Chemistry, University of Wisconsin, Madison, Wisconsin 53706, Institut für Physikalische Chemie, Lehrgebiet A, Universität Hannover, D-30167 Hannover, Germany, Department of Chemistry, Merkert Chemistry Center, Boston College, Chestnut Hill, Massachusetts 02467, and Department of Chemistry, University of Michigan, Ann Arbor, Michigan 48109

Received December 8, 2004; E-mail: mcMahon@chem.wisc.edu

Abstract: Polycyclic aromatic hydrocarbons (PAHs) have long been postulated as constituents of the interstellar gas and circumstellar disks. Observational infrared emission spectra have been plausibly interpreted in support of this hypothesis, but the small (or zero) dipole moments of planar, unsubstituted PAHs preclude their definitive radio astronomical identification. Polar PAHs, such as corannulene, thus represent important targets for radio astronomy because they offer the possibilities of confirming the existence of PAHs in space and revealing new insight into the chemistry of the interstellar medium. Toward this objective, the high-resolution rotational spectrum of corannulene has been obtained by Fourier transform microwave spectroscopy, and the dipole moment (2.07 D) of this exceptionally polar PAH has been measured by exploiting the Stark effect.

Introduction

Fundamental questions concerning the nature and composition of interstellar space, circumstellar envelopes, and planetary atmospheres manifest themselves at a fascinating intersection of astronomy, spectroscopy, and chemistry.^{1–6} The combination of laboratory spectroscopy and radio astronomy provides a powerful capability for the detection and identification of molecular species in the interstellar medium (ISM). Rotational transitions for molecular species occur across an extremely wide frequency range (1–1000 GHz), and the transitions can be measured with remarkably high precision (one part in 10⁸). As a consequence, the detection of just a few rotational transitions by radio astronomy represents a unique “fingerprint” and the basis for a secure spectroscopic assignment.⁷ A total of 129 molecules have been detected in interstellar space; 114 have been detected by radio astronomy and the remaining 15 by

infrared or ultraviolet astronomy.⁸ The majority of these species are organic molecules, and these molecules comprise a diverse representation of organic functionality. Unfortunately, radio astronomy is not amenable to the detection of nonpolar, or weakly polar, species because microwave signal strength is proportional to the square of the molecular dipole moment. Notable blind spots, therefore, compromise our picture of the organic species in the interstellar medium. Despite the fact that numerous (polar) carbon-rich molecules have been detected in space, simple aromatic hydrocarbons, polycyclic aromatic hydrocarbons (PAHs), and fullerenes remain inaccessible to radio astronomy.

Infrared emissions have been detected from a variety of astronomical sources. One widely held, albeit controversial, interpretation ascribes some of these features to aromatic hydrocarbons.^{3,6,9} For example, an emission feature at 14.8374 μm (673.9732 cm^{-1}), recently observed using the Infrared Space Observatory (ISO), has been assigned as the ν_4 deformation mode of benzene.¹⁰ Careful laboratory spectroscopy of selected larger aromatic hydrocarbons, however, has not furnished agreement with astronomical observational data.¹¹ Fits of infrared emission spectra from mixtures of PAHs with observational data are persuasive, but infrared emission data are inherently less precise than those obtained by high-resolution

[†] National Institute of Standards and Technology.

[‡] University of Wisconsin.

[§] Universität Hannover.

[#] Boston College.

[⊥] University of Michigan.

^{*} Present Address: Department of Chemistry, University of Cincinnati, Cincinnati, OH 45221.

(1) Herbst, E. *Chem. Soc. Rev.* **2001**, *30*, 168–176.

(2) McCarthy, M. C.; Thaddeus, P. *Chem. Soc. Rev.* **2001**, *30*, 177–185.

(3) Ehrenfreund, P.; Charnley, S. B. *Annu. Rev. Astron. Astrophys.* **2000**, *38*, 427–483.

(4) *Chemistry and Physics of Molecules and Grains in Space*; Royal Society of Chemistry: London, 1998; Vol. 109.

(5) Winnewisser, G.; Herbst, E. *Rep. Prog. Phys.* **1993**, *56*, 1209–1273.

(6) Allamandola, L. J. *Top. Curr. Chem.* **1990**, *153*, 1–25.

(7) Burke, B. F.; Graham-Smith, F. *An Introduction to Radio Astronomy*, 2nd ed.; Cambridge University Press: Cambridge, U.K., 2002.

(8) Lovas, F. J. *J. Phys. Chem. Ref. Data* **2004**, *33*, 177–355.

(9) Léger, A.; Puget, J. L. *Astron. Astrophys.* **1984**, *137*, L5–L8.

(10) Cernicharo, J.; Heras, A. M.; Tielens, A. G. G. M.; Pardo, J. R.; Herpin, F.; Guélin, M.; Waters, L. B. F. M. *Astrophys. J.* **2001**, *546*, L123–L126.

(11) Schlemmer, S.; Cook, D. J.; Harrison, J. A.; Wurfel, B.; Chapman, W.; Saykally, R. J. *Science* **1994**, *265*, 1686–1689.

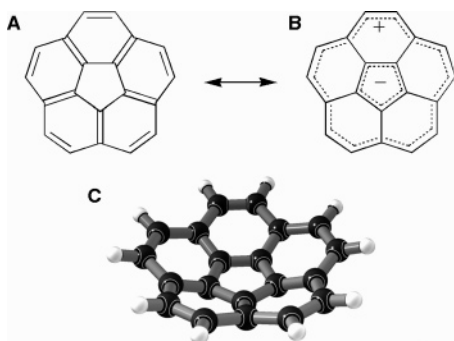


Figure 1. Corannulene, $C_{20}H_{10}$. (A) Line-bond structural representation. (B) Polar resonance structure. (C) Three-dimensional geometry determined by gas-phase electron diffraction.³²

rotational spectroscopy. Although the spectroscopic detection of aromatics, PAHs, and fullerenes may be equivocal, these species represent logical targets for study on the basis of the known, or presumed, chemistry of interstellar clouds and circumstellar environments. It is also worth noting that fullerenes^{12–14} and PAHs¹⁵ obtained from meteorites and interplanetary dust particles are unequivocally extraterrestrial in origin.

Against this backdrop, we initiated a series of investigations to develop the high-resolution laboratory rotational spectroscopy required to conduct astronomical searches for aromatic compounds and/or their chemical precursors or degradation products.^{16–18} In the current investigation, we describe the rotational spectrum of corannulene (Figure 1), a $C_{20}H_{10}$ PAH in which a unique combination of structural features is predicted to confer on the molecule an exceptionally large dipole moment of $\mu \approx 2.1$ D.¹⁹ The polarity of this molecule arises from strain-induced pyramidalization of the carbon atoms in the central five-membered ring, which causes the polycyclic network to adopt a nonplanar, bowl-shaped geometry (Figure 1C). The carbon atoms comprising the outer rim of the bowl lie 0.87 Å above the plane of the central ring.^{20,21} Superimposed on this curved geometry, an electronic structure of corannulene derived from simple organic resonance theory pictures the molecule as an anionic five-membered ring core, with six π electrons, and a cationic 15-membered outer rim, containing 14 π electrons (Figure 1B).²² The two oppositely charged conjugated cycles in this picture both satisfy the classical definition of Hückel aromaticity ($4n + 2$ π electrons).

The synthesis of corannulene by Barth and Lawton in 1966 was a landmark in aromatic hydrocarbon chemistry;^{22,23} that preparation of the first geodesic polyarene preceded, by more

than 20 years, developments associated with other “curved aromatics” (fullerenes, carbon nanotubes, and buckybowls). More recently, corannulene has been discovered, along with dozens of planar polycyclic aromatic hydrocarbons and fullerenes, in a variety of hydrocarbon flames.^{24,25} In contrast to planar polycyclic aromatic hydrocarbons and fullerenes, however, the nonplanar corannulene is polar and thus amenable to characterization by high-resolution rotational spectroscopy. A polar PAH represents a profoundly significant target for astronomical detection, one that offers the possibility to fill an important void in our understanding of the chemistry of interstellar space and an opportunity to confirm the existence of extraterrestrial PAHs.

Methods

Spectral survey scans of the rotational spectrum of corannulene were obtained using a high-resolution Fourier transform microwave (FTMW) spectrometer, a pulsed-molecular-beam Fabry–Pérot cavity spectrometer of the Balle–Flygare design.^{26,27} The sample of corannulene was prepared by the method described previously.²⁸ Corannulene is a solid at room temperature; it sublimates at 170 °C (0.02 Torr) and melts at 268–269 °C (under nitrogen).²² To obtain sufficient vapor pressure to record the rotational spectrum, the sample was heated in a reservoir nozzle installed in the backside (atmospheric pressure side) of the integral end flange-mirror of the FTMW spectrometer at NIST.²⁷ Most measurements were carried out at a nozzle temperature between 220 and 250 °C and at a carrier gas pressure near 140 kPa (80%/20% mixture by volume of neon and helium). All frequency measurements were referenced to a rubidium frequency standard. The spectrometer used for the Stark-effect measurements at Hannover also utilizes a coaxially oriented beam-resonator arrangement (COBRA), that is, the molecular jet expands coaxially to the axis of the near-confocal Fabry–Pérot-type resonator.²⁹ The principal advantage of the longer transit time of the molecular jet in the coaxial arrangement becomes applicable for Stark-effect experiments where very narrow line widths are desired.³⁰ The direction of the electric Stark field is perpendicular to the polarized microwave field, leading exclusively to the selection rules $\Delta M_J = \pm 1$. The electric field, E , was determined by calibration measurements with the $OC^{36}S$ and ^{18}OCS isotopomers of OCS using a dipole moment of $\mu = 0.71519(3)$ D.³¹

The initial survey search scans were carried out in the frequency range of 12.0–12.4 GHz, starting at a nozzle temperature of ~ 180 °C and repeating the scan at higher temperatures up to 240 °C. For each spectral scan, 25 free induction decays were averaged and Fourier transformed at stepped frequency intervals of 0.5 MHz and pulse repetition rates of 5 Hz. The frequency range was chosen for optimum sensitivity of the spectrometer, with a foreknowledge of the predicted frequency for the $J = 12 \leftarrow 11$ transition. The rotational constant calculated from the structure reported by Hedberg et al.³² guided the search: $B = 508.192$ MHz. The $J = 12 \leftarrow 11$ transition was observed near 12 236 MHz and was readily verified by observing the nearly equally spaced transitions above and below this frequency. All of the observed transitions are listed in Table 1. The four lowest frequencies were obtained in Hannover during the course of Stark-effect measure-

- (12) Becker, L.; Bunch, T. E.; Allamandola, L. J. *Nature* **1999**, *400*, 227–228.
 (13) Becker, L.; Poreda, R. J.; Bunch, T. E. *Proc. Natl. Acad. Sci. U.S.A.* **2000**, *97*, 2979–2983.
 (14) Poreda, R. J.; Becker, L. *Astrobiology* **2003**, *3*, 75–90.
 (15) Clemett, S. J.; Maechling, C. R.; Zare, R. N.; Swan, P. D.; Walker, R. M. *Science* **1993**, *262*, 721–725.
 (16) McMahon, R. J.; Halter, R. J.; Fimmen, R. L.; Wilson, R. J.; Peebles, S. A.; Kuczkowski, R. L.; Stanton, J. F. *J. Am. Chem. Soc.* **2000**, *122*, 939–949.
 (17) Halter, R. J.; Fimmen, R. L.; McMahon, R. J.; Peebles, S. A.; Kuczkowski, R. L.; Stanton, J. F. *J. Am. Chem. Soc.* **2001**, *123*, 12353–12363.
 (18) McMahon, R. J.; McCarthy, M. C.; Gottlieb, C. A.; Dudek, J. B.; Stanton, J. F.; Thaddeus, P. *Astrophys. J.* **2003**, *590*, L61–L64.
 (19) Baldrige, K. K.; Siegel, J. S. *Theor. Chem. Acc.* **1997**, *97*, 67–71.
 (20) Hanson, J. C.; Nordman, C. E. *Acta Crystallogr.* **1976**, *B32*, 1147–1153.
 (21) Seiders, T. J.; Baldrige, K. K.; Grube, G. H.; Siegel, J. S. *J. Am. Chem. Soc.* **2001**, *123*, 517–525.
 (22) Barth, W. E.; Lawton, R. G. *J. Am. Chem. Soc.* **1971**, *93*, 1730–1745.
 (23) Barth, W. E.; Lawton, R. G. *J. Am. Chem. Soc.* **1966**, *88*, 380–381.

- (24) Lafleur, A. L.; Howard, J. B.; Marr, J. A.; Yadav, T. J. *Phys. Chem.* **1993**, *97*, 13539–13543.
 (25) Richter, H.; Grieco, W. J.; Howard, J. B. *Combust. Flame* **1999**, *119*, 1–22.
 (26) Balle, T. J.; Flygare, W. H. *Rev. Sci. Instrum.* **1981**, *52*, 33–45.
 (27) Suenram, R. D.; Grabow, J. U.; Zuban, A.; Leonov, I. *Rev. Sci. Instrum.* **1999**, *70*, 2127–2135.
 (28) Scott, L. T.; Cheng, P.-C.; Hashemi, M. M.; Bratcher, M. S.; Meyer, D. T.; Warren, H. B. *J. Am. Chem. Soc.* **1997**, *119*, 10963–10968.
 (29) Grabow, J.-U.; Stahl, W.; Dreizler, H. *Rev. Sci. Instrum.* **1996**, *67*, 4072–4084.
 (30) Schnell, M.; Banser, D.; Grabow, J.-U. *Rev. Sci. Instrum.* **2004**, *75*, 2111–2115.
 (31) Reinartz, J. M. L. J.; Dymanus, A. *Chem. Phys. Lett.* **1974**, *24*, 346–351.
 (32) Hedberg, L.; Hedberg, K.; Cheng, P.-C.; Scott, L. T. *J. Phys. Chem. A* **2000**, *104*, 7689–7694.

Table 1. Calculated and Measured Rotational Transitions for Corannulene (C₂₀H₁₀)

transition $J \leftarrow J''$	calculated frequency ^a (MHz)	measured frequency ^b (MHz)	energy lower state (cm ⁻¹)
1-0	1019.6854(1)		0.000
2-1	2039.3706(1)		0.034
3-2	3059.0556(2)		0.102
4-3	4078.7404(2)		0.204
5-4	5098.4247(2)	5098.4246(5)	0.340
6-5	6118.1084(3)	6118.1081(5)	0.510
7-6	7137.7916(3)	7137.7916(5)	0.714
8-7	8157.4740(3)	8157.4739(5)	0.952
9-8	9177.1556(3)	9177.156(2)	1.224
10-9	10196.8363(4)	10196.838(2)	1.531
11-10	11216.5159(4)	11216.517(2)	1.871
12-11	12236.1943(4)	12236.197(2)	2.245
13-12	13255.8715(5)	13255.872(2)	2.653
14-13	14275.5473(6)	14275.549(2)	3.095
15-14	15295.2217(7)	15295.222(2)	3.571
16-15	16314.8945(8)	16314.894(2)	4.082
17-16	17334.5657(10)	17334.564(2)	4.626
18-17	18354.2350(12)	18354.234(2)	5.204
19-18	19373.9025(15)	19373.903(2)	5.816
20-19	20393.5680(18)		6.462
21-20	21413.2314(21)		7.143
22-21	22432.8926(25)		7.857
23-22	23452.5515(29)		8.605
24-23	24472.2080(33)		9.388
25-24	25491.8619(39)		10.204

Parameters:^a
B 509.842684(27) MHz
D_J 0.004356(76) kHz
 μ 6.908(60) × 10⁻³⁰ Cm
 2.071(18) D

^a Uncertainties shown in parentheses are type-A expanded uncertainties³⁷ with a coverage factor $k = 2$ (two standard deviations). ^b Uncertainties shown in parentheses are estimated type-B with a coverage factor $k = 1$.

ments. Since corannulene is an oblate symmetric top, it could exhibit K structure; however, no splittings were observed.

Results and Data Analysis

The energy levels of an oblate symmetric top may be described by eq 1:

$$W = BJ(J+1) + (C-B)K^2 - D_J J^2(J+1)^2 - D_{JK} J(J+1)K^2 - D_K K^4 \quad (1)$$

and the transition frequency is described by eq 2:

$$\nu(\Delta K = 0, J \rightarrow J+1) = 2B(J+1) - 4D_J(J+1)^3 - 2D_{JK}(J+1)K^2 \quad (2)$$

where J is the lower state rotational quantum number, B the rotational constant, and D_{JK} and D_J are centrifugal distortion terms. Since no K structure was observed, D_{JK} cannot be determined.³³ The measurements listed in Table 1 were the least-squares fit to two parameters of eq 2 with the resulting B and D_J values shown at the bottom of Table 1. Table 1 also includes calculated frequencies for all transitions up to $J = 25$ (25 GHz) as a convenience for subsequent laboratory or astronomical measurements. Table S1 (Supporting Information) carries the calculations up to $J = 154$ (158 GHz).

For Stark-effect measurements, it is desirable to limit the number of M_J components such that an assignment and analysis becomes feasible. Thus, low J transitions are preferred, which

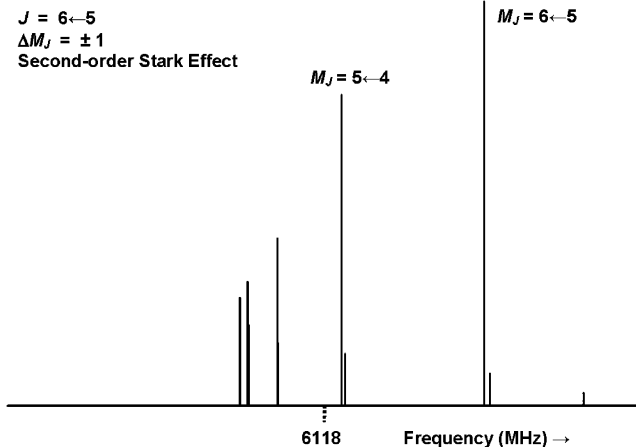


Figure 2. Predicted second-order Stark pattern for $K = 0$ of the $J = 6 \leftarrow 5$ transition of the symmetric top C₂₀H₁₀ with the selection rule $\Delta M_J = \pm 1$.

also coincides with the boundary conditions introduced by the rotational temperature of the species in the supersonic jet expansion. With a temperature as low as 1 K, only rotational levels with very low J values are occupied. Transitions involving low J values are especially valuable when using coaxially aligned electrodes for Stark effect applied in resonators (CAESAR) since the selection rule of $\Delta M_J = \pm 1$ gives rise to approximately twice the number of M_J components as compared to the common parallel plate arrangement with $\Delta M_J = 0$. On the other hand, the small B constant (509.8 MHz) means that the low J transitions will occur at frequencies where the diffraction losses of the Fabry–Pérot resonator are not negligible. This limits the usable J transitions to a very narrow range. In these experiments, the $J = 9 \leftarrow 8$ transition was inaccessible, while the intensity of the $J = 8 \leftarrow 7$ transition was weak. The $J = 6 \leftarrow 5$ and $J = 7 \leftarrow 6$ transitions, which both lie within the sensitive frequency range of the instrument, are predicted to exhibit strong M_J components (one and two, respectively) that display a large Stark shift toward higher frequency (positive shift), as well as one strong M_J component that displays a positive, but rather small effect upon the application of an electric field. All other components with positive shift are rather weak, while the components with negative shift show only a small displacement from one another and, thus, are poorly resolved. Figure 2 depicts the predicted Stark-splitting pattern for the $J = 6 \leftarrow 5$ transition.

An analysis of the Stark effect of the selected components turned out to be straightforward even though the total number of M_J components is still large. Figure 3 provides amplitude spectra of the observed Stark-split and -shifted $M_J = 6 \leftarrow 5$ and $M_J = 5 \leftarrow 4$ components of the $J = 6 \leftarrow 5$ transition for different electric fields. Other M_J components seen in the spectrum have not been analyzed either because of their much smaller intensity or because individual components were not resolved. The analysis is based on eq 3, giving the Stark shifts, $\Delta\nu$, that are valid for $K = 0$ and the selection rule $\Delta M_J = \pm 1$.

$$\Delta\nu(\Delta M_J = \pm 1, J \rightarrow J+1) =$$

$$\frac{\mu^2 E^2}{2h^2 B} \left[\frac{(J+1)(J+2) - 3(M_J \pm 1)^2}{(J+1)(J+2)(2J+1)(2J+5)} - \frac{J(J+1) - 3M_J^2}{J(J+1)(2J-1)(2J+3)} \right] \quad (3)$$

(33) Details available as Supporting Information.

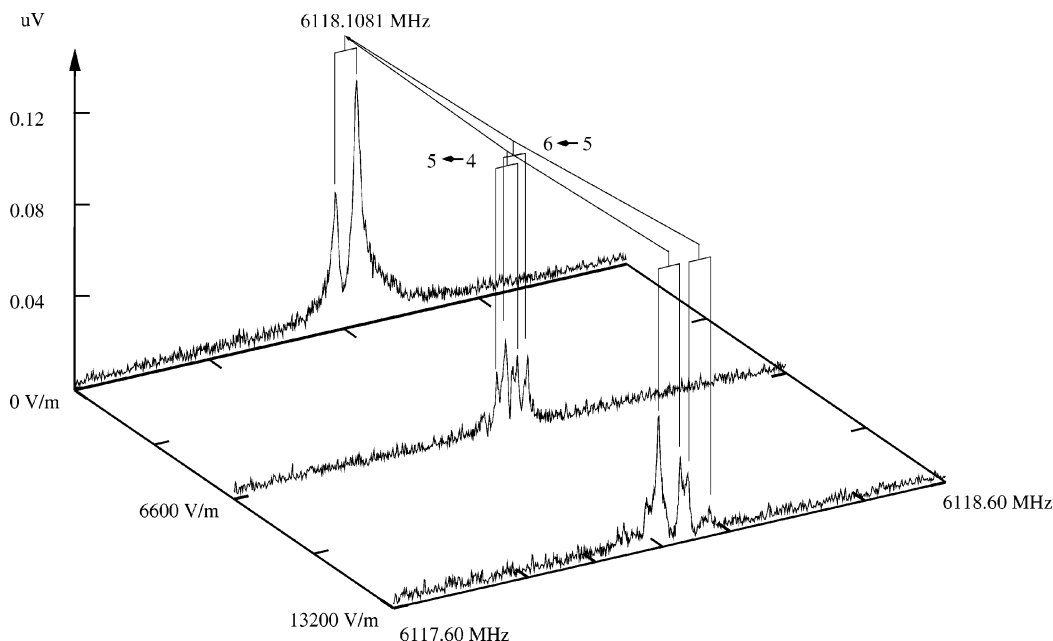


Figure 3. Observed line splittings of the $J = 6 \leftarrow 5$ transition of $C_{20}H_{10}$ in an electric field of 0.0, 6.6, and 13.2 kV/m. Coupling bars indicate a doublet splitting of 37.9 kHz caused by the Doppler effect of the 928 m/s molecular jet expanding along the resonator axis.

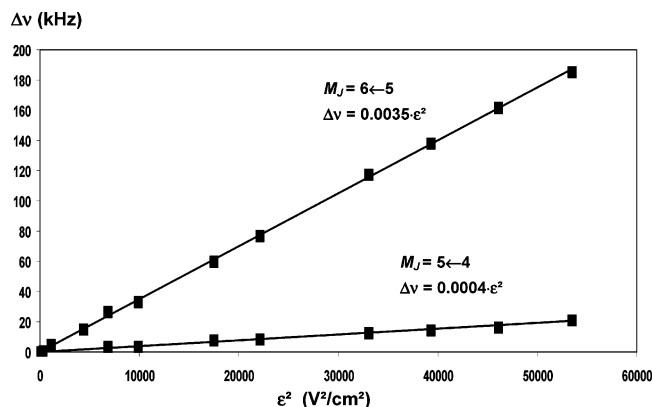


Figure 4. Observed line shifts ($\Delta\nu$) versus the square of the electric field (ϵ^2) for the $M_J = 6 \leftarrow 5$ and $M_J = 5 \leftarrow 4$ components of the $J = 6 \leftarrow 5$, $K = 0$ transition of $C_{20}H_{10}$.

with J and M_J at the lower state values. Expressions for the $M_J = 6 \leftarrow 5$ and $M_J = 5 \leftarrow 4$ components of the $J = 6 \leftarrow 5$ transition may be obtained from eq 3. From these expressions, we determined a dipole moment for corannulene of $\mu = 6.908(67) \times 10^{-30}$ Cm ($\mu = 2.071(20)$ D) from the $M_J = 6 \leftarrow 5$ component and $\mu = 6.85(18) \times 10^{-30}$ Cm ($\mu = 2.055(54)$ D) from the $M_J = 5 \leftarrow 4$ component. A global fit of all measurements (Figure 4) yields a dipole moment for corannulene of $\mu = 6.908(60) \times 10^{-30}$ Cm ($\mu = 2.071(18)$ D), a value that stands in remarkably good agreement with the best computational estimate of ca. 2.1 D.¹⁹

Discussion

The corannulene microwave spectrum is a textbook example of a rigid oblate symmetric top. The measured B value exhibits good agreement (within 0.3%) with the value calculated from the structural parameters determined in a gas-phase electron diffraction/computational study.³² In the current study, the values of B and D_J are determined with sufficient precision to be useful for radio astronomy. Structural details, such as C–C bond distances, however, cannot be obtained without additional

spectral data from isotopic species, such as a monosubstituted ^{13}C species. Although there are 10 equivalent carbons in the outer rim of corannulene, which increases the effective natural abundance isotopic incorporation of ^{13}C at this site to approximately 9%, mono- ^{13}C incorporation lowers the symmetry of the molecule to that of an asymmetric top, which splits the transitions and consequently reduces their intensity. The modest intensity of the spectrum of the normal isotopomer has precluded identification of the mono- ^{13}C isotopomer in natural abundance at this time.

Despite the pronounced deviation of corannulene from planarity, the barrier for its bowl-to-bowl inversion is modest (free energy barrier of 10.2 kcal/mol in solution at 209 K).^{21,34} The current FTMW measurements reveal no evidence for inversion splitting in the rotational transitions of corannulene. On the basis of the smallest line width observed experimentally, the inversion frequency must be below 5 kHz at the temperature of the measurement (< 2 K).³³ The small distortion constant ($D_J = 0.00436$ kHz) is consistent with that of a rigid aromatic structure, as opposed to a floppy (inverting) structure.

Corannulene ($C_{20}H_{10}$, molecular weight of 250 amu) is considerably larger than any of the known interstellar molecules, with the largest linear species being cyanopolyynes ($HC_{11}N$)⁸ and the largest nonlinear species being benzene (C_6H_6).¹⁰ Thus, observation of corannulene in interstellar sources would represent a substantial leap forward. Two types of interstellar sources might be considered to be promising places to look for corannulene, cold dark clouds and asymptotic giant branch (AGB) stars. If corannulene was present in a cold dark cloud, then the centimeter wavelength region (i.e., low J) would be the logical region to prospect, whereas a hot source would likely be more profitably examined at millimeter wavelengths (i.e., high J). A preliminary survey of published radio astronomy data from several sources^{8,35,36} yielded no matches between any of the unidentified lines (U-lines) and the frequencies of coran-

(34) Scott, L. T.; Hashemi, M. M.; Bratcher, M. S. *J. Am. Chem. Soc.* **1992**, *114*, 1920–1921.

nulene, but our new data now make possible a more deliberate search, aimed specifically at corannulene.

Summary

The existence of aromatic compounds in space remains a great, unresolved question at this time, and it is one that must be resolved in order to advance our understanding of the chemistry of the interstellar medium. In this study, we articulate a new strategy for probing the existence of polycyclic aromatic hydrocarbons (PAHs) in interstellar space, and we provide the laboratory spectroscopy that is required to implement this strategy. Our strategy identifies polar PAHs as targets for radio astronomy; plausible targets include nonplanar PAHs (“bucky-bowls”) as well as planar PAHs that contain polar substituents or heteroatoms. The current investigation of corannulene, a

nonplanar PAH (Figure 1), provides the gas-phase microwave rotational spectrum and the molecular dipole moment ($\mu = 2.071$ D). Efforts to conduct a directed radio astronomical search for corannulene are currently underway.

Acknowledgment. We gratefully acknowledge support from the National Science Foundation (R.J.M., L.T.S.), Department of Energy (L.T.S.), Deutsche Forschungsgemeinschaft, Land Niedersachsen (J.-U.G), and Fonds der Chemischen Industrie (M.S.). We thank R. J. Lavrich (EPA), J. F. Stanton (University of Texas), and M. J. Tubergen (Kent State University) for helpful discussions.

Supporting Information Available: Detailed discussion of centrifugal distortion constants and spectroscopic consequences of conformational bowl inversion. Table of calculated and measured rotational transitions up to $J = 154$ (158 GHz). This material is available free of charge via the Internet at <http://pubs.acs.org>.

- (35) Kaifu, N.; Ohishi, M.; Kawaguchi, K.; Saito, S.; Yamamoto, S.; Miyaji, T.; Miyazawa, K.; Ishikawa, S.-I.; Noumaru, C.; Harasawa, S.; Ocuda, M.; Suzuki, H. *Publ. Astron. Soc. Jpn.* **2004**, *56*, 69–173.
- (36) Goicoechea, J. R.; Cernicharo, J.; Pardo, J. R.; Guélin, M.; Phillips, T. G. *The Promise of the Herschel Space Observatory*; European Space Association, 2001; Vol. SP-460.
- (37) Taylor, B. N.; Kuyatt, C. E. *NIST Technical Note 1297* **1994**.

JA0426239